

# Morpho: A Self-deformable Modular Robot Inspired by Cellular Structure

Chih-Han Yu<sup>\*,§</sup> Kristina Haller<sup>†</sup> Donald Ingber<sup>‡,\*,§</sup> Radhika Nagpal<sup>\*,§</sup>  
chyu@fas.harvard.edu khaller@gmail.com donald.ingber@childrens.harvard.edu rad@eecs.harvard.edu

<sup>\*</sup>School of Engineering & Applied Sciences, Harvard University, Cambridge, MA, USA

<sup>†</sup>Department of Mechanical Engineering, MIT, Cambridge, MA, USA

<sup>‡</sup>Harvard Medical School & Children’s Hospital, Boston, MA, USA

<sup>§</sup>Harvard Institute for Biologically Inspired Engineering, Cambridge, MA, USA

**Abstract**—We present a modular robot design inspired by the creation of complex structures and functions in biology via *deformation*. Our design is based on the *Tensegrity* model of cellular structure, where active filaments within the cell contract and expand to control individual cell shape, and sheets of such cells undergo large-scale shape change through the cooperative action of connected cells. Such deformations play a role in many processes, e.g. early embryo shape change and lamprey locomotion. Modular robotic systems that replicate the basic deformable multicellular structure have the potential to quickly generate large-scale shape change and create dynamic shapes to achieve different global functions.

Based on this principle, our design includes four different modular components: (1) active links, (2) passive links, (3) surface membranes, and (4) interfacing cubes. In hardware implementation, we show several self-deformable structures that can be generated from these components, including a self-deformable surface, expandable cube, terrain-adaptive bridge [1]. We present experiments to demonstrate that such robotic structures are able to perform real time deformation to adapt to different environments. In simulation, we show that these components can be configured into a variety of bio-inspired robots, such as an amoeba-like robot and a tissue-inspired material. We argue that self-deformation is well-suited for dynamic and sensing-adaptive shape change in modular robotics.

## I. INTRODUCTION

Modular Robots are a class of robots that are composed of many homogeneous or heterogeneous modules that can coordinate to change the overall shape of the robot. The design and control of modular robots has been widely influenced by multicellular behaviors in biological systems, from module design to tasks like self-repair and self-replication [2]. Several research groups have demonstrated sophisticated mechanical designs that allow modular robots to transform their shape through changing the connectivity of modules [3], [4]. This process usually involves either self-reconfiguration (modules actively attaching, detaching, and moving to assume different positions) or self-assembly (modules moving via external vibrations or forces and selectively attaching). One can think of these processes as analogous to creating shapes by cell migration, cell growth, and even cell death in biology. The rearrangement of connectivity allows one to achieve a large range of shapes, even from a few modules. However, the shape change process is often slow in hardware implementation.

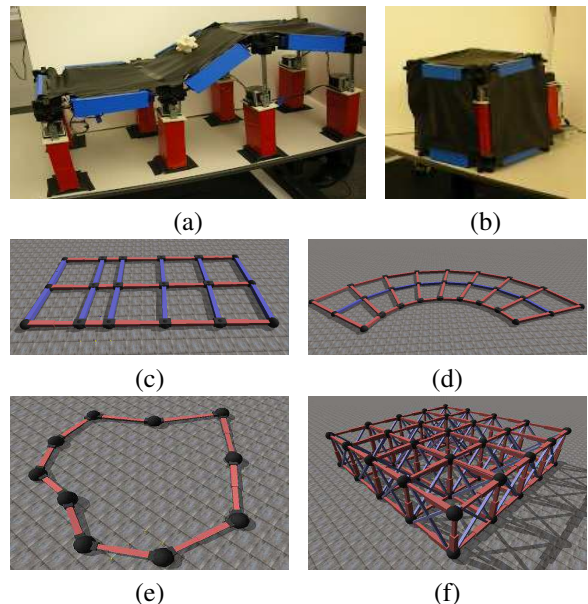


Fig. 1. Several example robots that can be generated from Morpho: (a) Flexible surface structure that can transport an object (b) Deformable cubic structure (c) Bio-inspired robot that can perform locomotion (d) Robotic structure that can perform dramatic shape deformation (e) Amoeba-like robot that dynamically changes its shape (f) Tissue-inspired programmable material. (a) – (b) are real hardware implementations; (c) – (f) are ODE simulations.

*Self-deformation* is another shape changing process observed in multicellular biological systems. Unlike growth and migration, this depends on a fixed connected topology of cells where individual cells exert actuation forces (expansion, compression) on the whole structure. This type of multicellular behavior can create complex shapes and achieve complex functions: e.g. gut formation in early animal embryos, contractions in the heart, traveling waves in the intestines, and locomotion in lampreys and manta rays. Ingber et al have proposed a *Tensegrity-like* model [5], [6], of how individual cells and multicellular tissues achieve this shape change, through the control of contractile filaments embedded in each cell. This model of shape change has been explored in depth in biology literature [7].

Modular robotic systems that replicate the basic de-

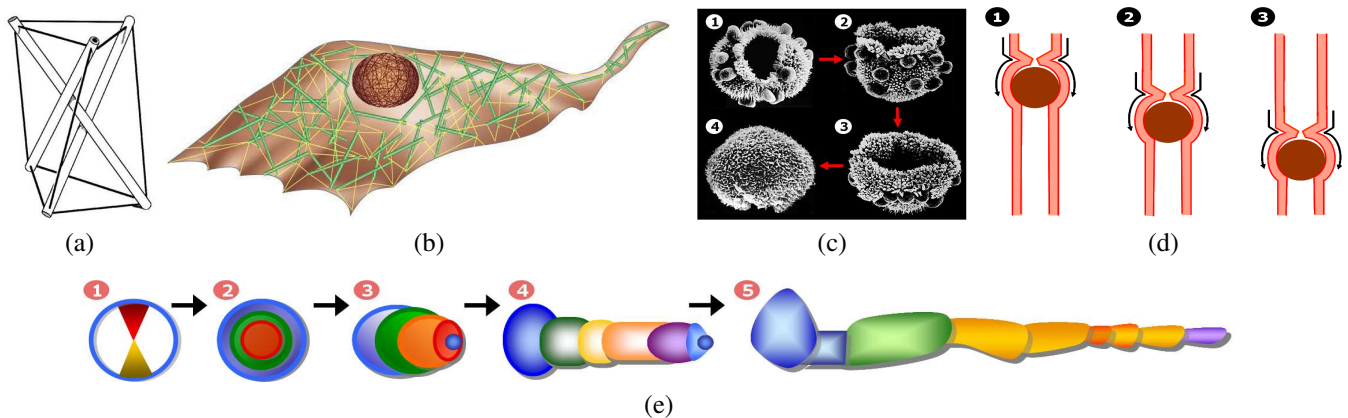


Fig. 2. Self-deformation in biology: (a) The Tensegrity structure. The model provides an explanation of how cells get their shapes. (b) A cell and its contractile filaments (colored green), which provide inner pulling force (photo courtesy of Matt Pickett). (c) The volvox algae form a hollow spherical colony that can invert itself through local contractions of individual cells (photo courtesy of David Kirk and Ichiro Nishii). (d) Peristaltic waves in the esophagus are achieved through distributed contraction of cells. (e) The imaginal disc of a fruit fly transforms from a flat sheet to a more complex 3D shape, a leg.

formable multicellular structure have the potential to quickly generate large-scale shape change and create time-varying shapes to achieve different global functions. However, self-deformation has only been explored to a limited extent in modular robotics; e.g. chain-based modular robots which use module angle change to create locomotion and shape change but also rely on attachment/detachment [8], [9], [10]. Only recently have robots based on contracting linear modules been explored [11]. Our research is inspired by this recent work. We seek to define a modular robot system aimed at exploring shape change through self-deformation.

In this paper, we present a self-deformable modular robot design. Our design is based on the Tensegrity model of cellular structure, where active filaments within the cell contract and expand to control individual cell shape, and the forces between connected cells create shape change within the tissue. Our system incorporates four different modular components: (1) *active links*: linear structures whose overall length can be controlled. (2) *passive links*: linear structures that can be passively compressed or expanded. (3) *surface membranes*: square structures that are capable of expanding. (4) *interfacing cubes*: an connector that can interface with passive/active links and surface membranes. We show that with different combinations and connections between the four components, many robotic configurations can be created, including two dimensional surfaces, volumetric structures, and several bio-inspired robots.

We demonstrate three prototypes in hardware that can be achieved within this framework: a deformable surface that is capable of transporting an object, a terrain-adaptive bridge structure previously proposed in [1], and a volumetric cube that changes its size (Fig. 1 (a) and (b)). We show that the terrain-adaptive bridge is able to quickly adapt to terrains with different roughness levels using tilt sensors mounted on the passive links. We also simulate the dynamics of these modules in Open Dynamics Engine (ODE) and generate more complex bio-inspired robots in order to replicate biological behaviors. The examples include a bio-inspired

robot that locomotes using shape deformation and a tissue-inspired programmable material proposed in [12] (Fig. 1 (c) – (f)). Finally, we discuss potential applications and future work that can be achieved with this framework. We envision the proposed self-deformable system being used to study the benefits and disadvantages of self-deformation vs. other types of self-assembly.

The remainder of the paper is organized as follows. We present related work and biological inspiration in Section II. The detailed design of our Morpho modular robot is described in Section III. We present several different applications/structures and that can be achieved within this framework and real hardware experiments in Section IV. We demonstrate simulations of several bio-inspired robots in Section V. Finally, we provide several potential applications VI and conclusions in Section VII.

## II. MOTIVATION AND RELATED WORK

Our research is inspired by the complex biological structures that are formed through deformation (Fig. 2). At the most basic level, a cell can be thought of as an active Tensegrity structure [6], where individual micro-filaments coordinate to dramatically change the shape of the cell (as shown in Fig. 2 (a) and (b)) and even create locomotion (e.g. in ameoba). When many such cells link together to form multicellular tissues, organs, or organisms, they can coordinate to create complex global transformations. For example, as shown in Fig. 2 (c), the volvox algae form a hollow spherical colony that can invert itself purely through local contractions of individual cells [13].

In animal development, deformation is a key part of the transformation from an ovoid embryo into a complex structure. For example, the formation of the gut and the neural tube are driven primarily by local shape changes in cells that form the the embryo surface [14]. This deformation transforms the hollow ovoid shape into a torus and concentric tubes. Even more dramatic is the stage of metamorphosis in the fruit fly, where a group of connected cells (called the

imaginal disc) transforms from a flat sheet to a complex 3D shape – including the wing, the leg, the antenna – just by folding and stretching deformations (Fig. 2 (e)). Finally, the function of many organs in the human body depend on multicellular tissues that can create time-varying shapes through deformation, e.g. the pumping of the heart or the peristolic waves in the esophagus (Fig. 2 (d)). Each cell in these multicellular muscle tissues has only limited actuation capability. However, through local coordination large-scale, rapid, and flexible transformation can be achieved. In many organisms, such as fish and snake, these distributed shape deformations are used to create complex and flexible locomotion behaviors [15], [16].

In modular robotics literature, there have been some examples of work inspired by shape change through deformation: the Crystalline robot [17], Tetrobot [18], the origami-inspired foldable sheet [12], the Deformatron robot [19], the environmentally-adaptive surface [1], and the Odin robot [11]. Our work is inspired by these previous examples (in particular [1], [11], [18]). We propose a heterogeneous modular system consisting of four general modules. These modules are analogous to the basic components in the Tensegrity model which can be composed in many ways to create a variety of surfaces and 3D volumetric structures, including many of the biological structures discussed previously. Tensegrity-based robots, along with their control and structural properties, have been previously explored in [20], [21]. In this paper, we further modularize the components of Tensegrity-based robots such that the same set of modules can be reconfigured into different Tensegrity-based structures.

Deformation-based shape change has some distinct advantages, both in biology and modular robots. Unlike growth [2] or rearrangement ([3], [4], [22], [23]) approaches in modular robotics, deformation can be achieved with much higher speeds. This makes it a likely candidate for time-varying/dynamic shapes or structures that are constantly adapting to the environment, however, there are limits to what can be achieved purely through deformation. Eventually it may be possible to combine the type of modules described here with "strut-based" self-assembly techniques such as the Shady3D robot [24] to allow both self-reconfiguration and self-deformation.

### III. MORPHO MODULAR ROBOT DESIGN

In this section, we describe the design of each component of Morpho. There are four different modular components, including *active links*, *passive links*, *interfacing cubes*, and *surface membranes*. Geometrically, the active/passive links can be viewed as lines, interfacing cubes can be viewed as points and surface membranes can be viewed as planes.

The main function of active links is to enable deformation of the structure by varying its physical length. Passive links allow the structure to resolve different geometries by passively expanding and contracting in accordance with the deformation generated by the active links. The surface membrane provides a flexible 3D plane to convert the skeleton

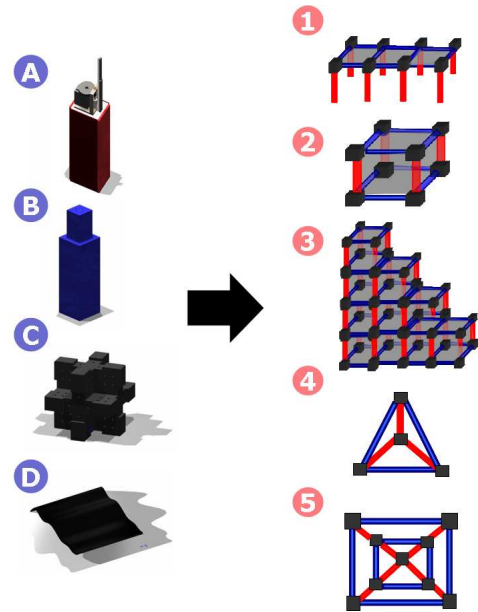


Fig. 3. Morpho has four different types of reconfigurable modules that can be combined to form structures like those shown on the right: (1) A surface structure capable of forming a terrain adaptive bridge or transporting an object. (2) – (3) A cubic structure capable of volumetric deformation. Cubes can be combined to form larger structures, such as a staircase. (4) – (5) Links can also be combined to form non-cubic structures, such as this tetrahedron and this pyramid (as viewed from above)

structure to a volume, when attached to other modules. This allows the structure to interact with objects and form deformable volumes. The interfacing cubes provide a connection mechanism for all of the other modular components.

As shown in Fig. 3, through different combinations and configurations of these modules we are capable of forming different types of 2D structures and 3D volumes, including surfaces, cubes, tetrahedrons, and compositions of those structures (Fig. 3 (1) – (5)). The Morpho modules are generic enough to be reconfigured into many bio-inspired robots. We will illustrate some of them in Section V. We will now provide a detailed description of each hardware element.

#### A. Active Link

The active links can controllably change the skeleton of the structure, as shown in Fig. 4 (a). The mechanical functionality of the active link is similar to a linear actuator. The main difference is that its physical length can be precisely controlled. In contrast, most linear actuators can only provide fully expanded/compressed configurations<sup>1</sup>. In addition, the active links are also equipped with connecting mechanisms to attach to interfacing cubes.

As shown in Fig. 4 (a), our current hardware implementation of an active link uses a AX-12+ servo. The AX-12+ provides position, speed, and load feedback. Each servo is connected to a large spur gear, coupled with a smaller spur gear, to increase the speed at which the links are able to move, giving the system an overall 1:6 gear ratio. The small

<sup>1</sup>an extra position sensor and controller are required for most linear actuators to achieve position control

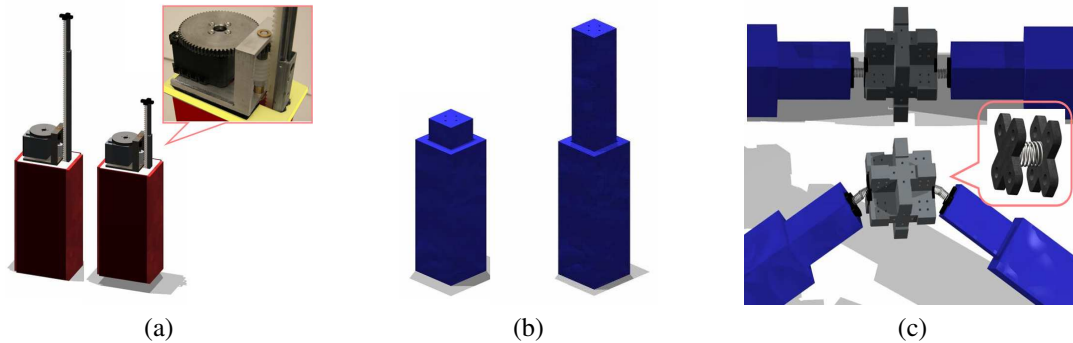


Fig. 4. (a) The expanded (left) and contracted (right) state of the red active links. Active links expand/contract when a servo drives a vertically mounted rack up/down. As they expand and contract they force (b) the blue passive links to contract and expand to accommodate new geometries. (c) Interfacing cubes are used to connect to links and membranes. Since some geometries require a change in the angle between a passive link and a connecting cube, the spring interface between the two gives extra flexibility.

spur gear is attached to a worm gear that raises and lowers a vertically mounted rack. These continuous rotation actuators allow the active links to expand and compress with an overall six inch height differential. The maximal torque an AX-12+ can generate is 16.5 kgf.cm, and this generates a maximal payload of 2 kg for a single active link. To further increase the speed of expansion and contraction we also reduced friction in the system by mounting the vertical rack on a ball-bearing slider. When the motor rotates at full speed the active link can be extended/compressed at the speed of 2 inch/sec. A given length can be precisely achieved.

### B. Passive Link

Passive links are components that can be expanded or contracted while active links perform actuation. These passive links provide a supporting framework for the surface membrane. The detailed design of the passive link is shown in Fig. 4 (b) Each link consists of two concentric rectangular shells. The inner shell has a larger step at the end that slides along the inner dimension of the outer shell, using it as a bearing surface. To reduce friction between moving components, the shells for both the passive and active links were made out of acrylic, which has a low friction coefficient and can be rapidly machined with a laser cutter.

### C. Interfacing Cube

The function of the universal interfacing cube is to provide convergence points for links. As shown in Fig. 4 (c), the interfacing cubes provide six different attachment points for both passive and active links in addition to eight different surface membrane attachment points along all major axes. This allows links to connect in different ways according to different geometries. The surface area to which the outer membrane attaches is maximized in order to provide more stability and keep the membrane in tension.

A flexible connector is used to attach passive and active links with the interfacing cubes, as seen in Fig 4 (c). The two cross pieces screw into the cube and link. The spring allows for two consecutive nodes to reach different heights without over-constraining the system while providing enough

restoring force to maintain linearity between the links and the connectors.

### D. Surface Membrane

The function of the surface membrane is to cover the 3D skeleton, changing the overall structure into a volume or a surface. Therefore, the material needs to be stretchable while maintaining rigidity. This allows the surface or volume to deform while maintaining its overall shape.

Material selection was based on its bulk modulus (a measure of elasticity) and Young's Modulus (a measure of rigidity). Neoprene provides enough rigidity to minimize deformation under external pressure and can be stretched up to 300% its original size. Another potential selection of material is latex, which can stretch up to 780% its original size. The surface membranes attach flexibly along the edges of the links as well as the interfacing cubes.

### E. Communication/Control

We built our communication structure and protocol on the existing communication framework of the AX-12+ actuators. The maximal communication speed of the AX-12+ actuators is around 1Mbps. The control algorithm is run on a laptop computer (2GHZ CPU) that simulates purely distributed control in our simulation environment. At each iteration, the simulator takes sensor input from the real robot through serial port interface. The control algorithm then computes control parameter (desired expansion or contraction length) for each active link (actuator). The control output is then sent to all active links through serial interface. This procedure allows the same control trajectory to be simultaneously executed in simulation and on the real robot.

### F. Simulation Environment

Our simulation environment is constructed with the Open Dynamics Engine (ODE) which can simulate the physics of Morpho in different configurations (as shown in Fig. 5 (a – d)). We note that ODE is not capable of simulating deformable material, like the surface membrane in our module components. In our simulation, we use a sequence of rigid objects to approximate the property of such materials.

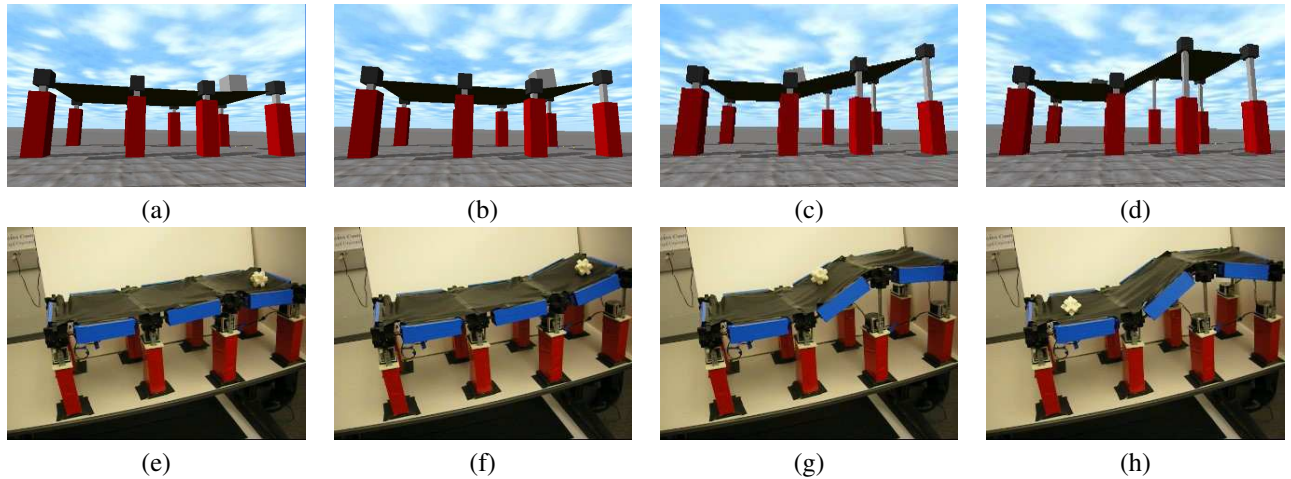


Fig. 5. (a-d) Control trajectories, computed in Open Dynamics Engine, of Morpho transporting a cubic object across three cells (e-h) the execution of computed control trajectories on the Morpho hardware platform.

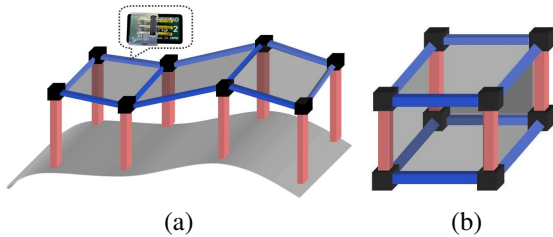


Fig. 6. Two different structures that can be achieved by reconfiguring the Morpho modules: (a) a bridge structure that can be used for such things as object transportation or terrain adaptation and (b) a cubic structure that can be used for volumetric deformation.

#### IV. EXPERIMENTS

In this section, we describe three experiments performed on the Morpho hardware platform. In the first experiment, we configure Morpho to form a flexible surface (Fig 6 (a)). The surface is programmed to be deformable, with the goal of transporting a cubic object from one side of the structure to the other. This allows us to examine Morpho’s ability to perform a task that requires fast shape deformation. In the second experiment, we examine its ability to perform an adaptation task, such as the terrain-adaptive bridge we simulate in [1]. The bridge structure is placed on a rough terrain, formed by bricks, and is programmed to maintain a level surface. The bridge surface, formed by passive links, is equipped with tilt sensors to sense the environment. In the third experiment, the modules are reconnected to form a cubical structure capable of volumetric expansion. This allows us to test Morpho’s deformability in different structures.

Our experimental results show that Morpho is capable of performing each of the tasks described above. It achieves fast shape formation while maintaining enough rigidity to allow an object to be transported between surface membranes efficiently. It adapts to rough terrain effectively and achieves a level surface when placed on terrains of different levels of roughness. The tasks are achieved after 40 iterations of our control algorithm. It can also perform volumetric

deformations with a 1.3 times increase in volume.

##### A. Object Transportation on Flexible Surface

In the first experiment, we perform object transport on a flexible surface. To construct the flexible surface, modules are connected as shown in Fig. 6 (a). The top surface is connected with passive links, spanned by three surface membranes to provide flexibility. Active links provide the vertical supports which can expand and contract to controllably deform the surface. The object being transported is a 2” × 2” × 2” ABS plastic cube.

We view each of the active links as a single agent. Each agent gets its neighborhood topology via message passing [12]. For every surface membrane an agent is connected to, it is programmed with the desired direction of transport to allow the object to reach the goal position. This allows us to implement a simple cooperation mechanism on them: when four such agents sense the object is in the surface connecting them, two of them will extend in order to roll the object in the direction of the goal.

These control trajectories are first computed in ODE simulation as shown in Fig. 5 (a – d), then executed on the Morpho. Fig. 5 (e – h) shows that the control trajectory successfully transports the object from the first cell to the third cell. The active links were capable of generating a 20 degree tilt angle in approximately three seconds, i.e. each cell was capable of deforming 1.3 times its original size in approximately three seconds. This allows us to successfully transport objects between surface membranes. This experiment shows that the design and construction of Morpho is capable of tasks that require fast shape-deformation, such as transporting an object (that is within weight limit) across a deformable surface. We further test the maximal payload of each cell. We discover that one limitation of our design is the surface membrane is not rigid enough to hold object that is more than  $\sim 3$  kg, although each active link is capable of lifting an object of 2 kg.

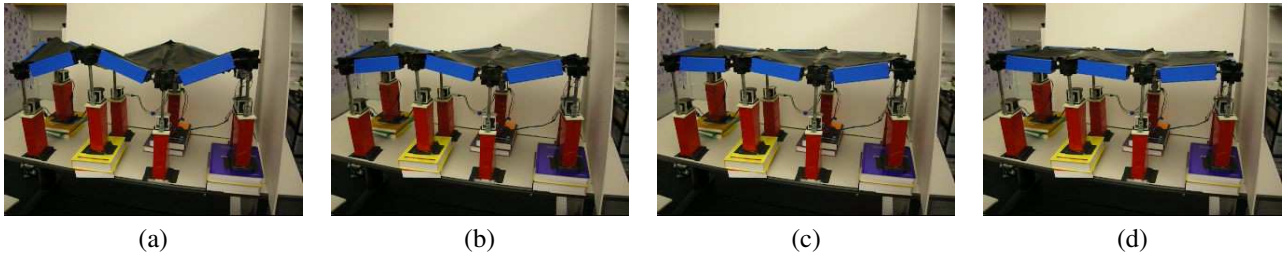


Fig. 7. (a-d) Morpho on rough terrain achieving a less than 3 degree tilt angle in 40 iterations of our control algorithm.

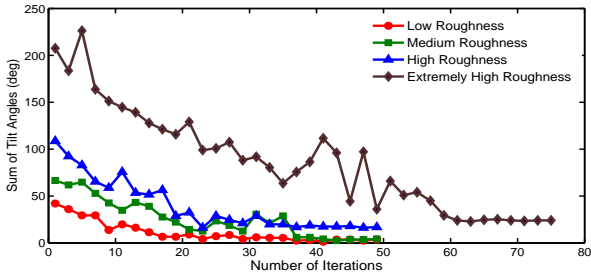


Fig. 8. The bridge structure’s response time to achieve its surface’s levelness. In low, medium, and high roughness cases, it is capable of achieving the average of passive links’ tilt angles  $\leq 3$  degree after 40 iterations. In extremely high roughness case, it achieves the same level of levelness after 60 iterations.

### B. Terrain-adaptive Bridge

In the second experiment, the modules were assembled in the same bridge-like configuration as the previous experiment (Fig 6 (a)). As shown in the figure, there is one passive link (blue) between each pair of neighboring active links (red). There is a tilt sensor, Kondo RAS-2 accelerometer, mounted on each passive link.

In this experiment, the assembly is placed on uneven terrain with the goal of achieving a flat top surface: this requires all tilt sensors to be zero. A decentralized algorithm for this task was previously proposed in [1]; we use it here to achieve the desired task. The active links are programmed as supporting groups in [1], while the passive links are programmed as surface groups. Connecting interfaces are treated as pivots. At each step, each surface group (passive link) senses and transmits its tilt angle to the neighboring pivots (connecting interface). Each pivot collects tilt sensor information from neighboring surface groups and computes the aggregated feedback. Each supporting group (active link) uses this information to control its actuation. The control algorithm run on each supporting group to change its height is shown as following:

$$h_i(t+1) = h_i(t) + \alpha \cdot \sum_{j \in N_i} \theta_{ij} \quad (1)$$

where  $h_i(t+1)$  is the height of  $i^{th}$  active link at next time step  $t+1$ ,  $N_i$  indicates the set of all neighbors of active link  $i$ , and  $\theta_{ij}$  is the tilt angle between link  $i$  and its neighbor link  $j$ .  $\alpha$  is a small constant between 0 and 1.

To test how fast the bridge can adapt to terrains of different roughness, we sequentially increase the roughness of the terrain by adding more bricks. Since the surface achieves levelness while all tilt sensor reading equal to zeros, we use the sum of all tilt sensor readings’ absolute values as our levelness measure  $\varepsilon$ , shown as the following equation:

$$\varepsilon = \sum_{\forall i, j \in N_i} \|\theta_{ij}\| \quad (2)$$

Fig. 7 (a) – (d), show a sample sequence of the self-adaptive tasks and Fig. 8 shows the number of iterations required to achieve levelness versus different levels of roughness of the underlying terrain. Since the tilt sensors we use are somewhat noisy, we define the bridge has achieve levelness when each passive link’s tilt angle is averagely smaller than 3 degree (10 passively links totally)

We can see from the Fig. 8 that the bridge surface is capable of achieving levelness after running the control algorithm for 40 iterations in low, medium, and high roughness cases (x axis represents the number of iterations and y axis is  $\varepsilon$ ). In extremely high roughness case, it achieves levelness after approximately 60 iterations. We refer the reader to [25] for the theoretical analysis of how such type of control algorithms (Eq. 1) scale with the difficulty of the tasks and the number of modules. This experiment indicates that the design and construction of the Morpho is suitable for self-adaptation tasks.

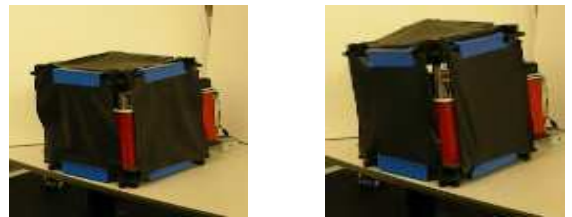


Fig. 9. Morpho configured into a cubic structure. In this configuration, with active links along one axis, the cube is capable of expanding to 1.3 times its original volume. Left: Original volume. Right: After expansion.

### C. Expandable Cube

In the third experiment, we test the Morpho modules configured into a cube, with passive links on two axes and active links on the third. Surface membranes are added to all six sides of the cube. We then perform a volumetric deformation task on the cubic structure as shown in Fig.

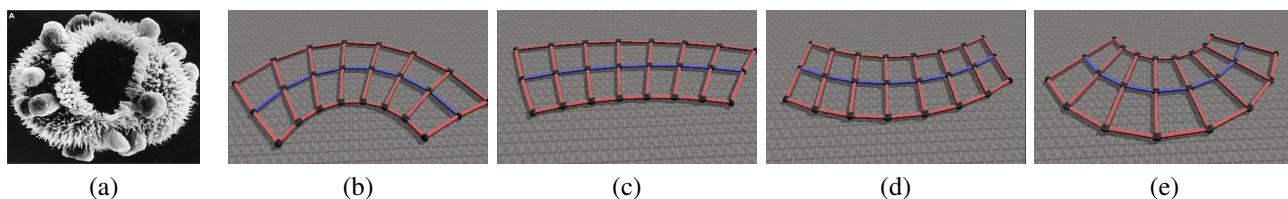


Fig. 10. (a) The volvox is a spherically shaped chlorophyte capable of inverting its geometry. (b) – (d) A sequence of simulations of the volvox structure. Inversion occurs as the outer arc of links contract and the inner arc of links expand.

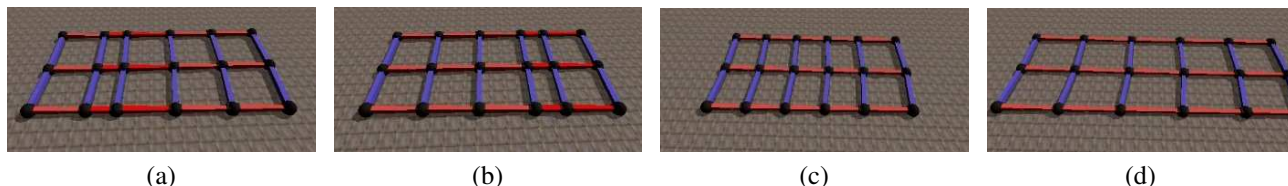


Fig. 11. A robotic structure that can perform locomotion by changing its shape. (a) – (b) The active links sequentially perform periodic motion; dark red links represent actuated links. (c) – (d) The robot traverse in horizontal direction by actuating active links simultaneously.

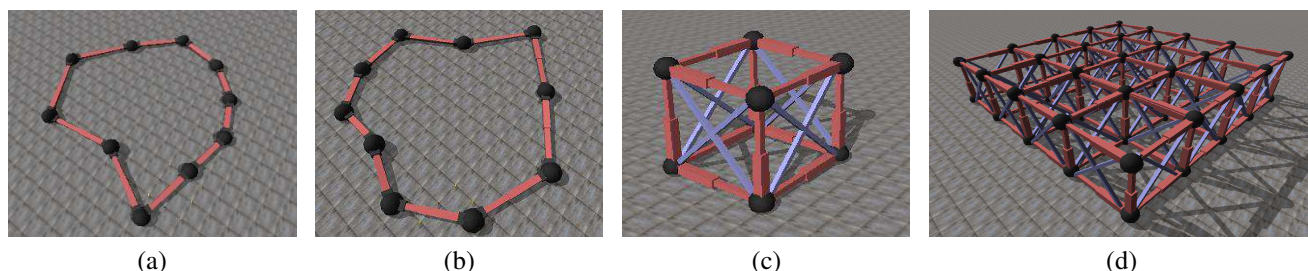


Fig. 12. (a) – (b) Amoeboid robot. The robot changes its shape while active links perform actuation. (c) A basic cube of the tissue-inspired programmable material (d) A programmable material that is formed by a grid of  $4 \times 4$  basic cubes.

6 (b). The active links expand, maximizing the volume of this configuration of modules.

Fig. 9 (a) and (b) show the volume of the cube before and after deformation. From the figure, the resulting volume is 1.3 times larger than the original volume. The stretchability of the surface membrane is the limiting factor in increasing the volume. With different materials and providing actuating links on all edges, (latex for example<sup>2</sup>), or a thinner piece of neoprene the volume could potentially expand up to 8 times its original volume before the length of the expanded links becomes the limiting factor.

## V. BIOLOGICALLY-INSPIRED ROBOTS

There are many interesting biological examples in nature that can perform self-deformation. Here we simulate dynamics of the Morpho modules with Open Dynamics Engine and illustrate several robots that mimic biological processes.

### A. Volvox Inversion

The volvox is a chlorophyte that takes the shape of a sphere. It is capable of inverting its geometry by expanding and contracting different areas along its perimeter, as shown in Fig. 10 (a). The Morpho, when configured appropriately, can reproduce this action. As shown in Fig. 10 (b), active

<sup>2</sup>In our preliminary experiment, some slimmer latex materials can be stretched to two times their original length. However, these materials are not as rigid as the Neoprene material we use in our experiments.

links are placed along the inner and outer perimeter, with concentric inner arcs composed of passive links. The cross struts are made from active links because throughout the inversion process they maintain a constant length instead of being passively stretched. Inversion will occur when the active links along the inner arc expand while the active links along the outer arc contract. Fig. 10 (b) – (d) shows a sequence of shapes generated by such collective actuation.

### B. Locomotion via Self-Deformation

There are many biological creatures that perform locomotion by changing their shapes. For example, inchworm and lamprey perform locomotion via periodic self-deformation. Here we illustrate a robotic structure that can perform locomotion via this self-deformation. As shown in Fig. 11, the horizontal links are placed with active links and the vertical links are placed with passive links. This configuration allows the robot to traverse along the horizontal direction while active links periodically contract and expand. Fig. 11 (a) and (b) show the case when active links sequentially perform such periodic actuation, and the robot is capable of performing locomotion. On the other hand, Fig. 11 (c) and (d) show the case when all active links simultaneous actuate.

### C. Amoeboid Robot

The amoeboid is a unicellular creature that can perform locomotion by transforming its shape. Our design is inspired

by [26], and the robot's perimeter are placed with active links. Two consecutive active links are connected with a interfacing cube. The design of the interfacing cubes allows the robot's shape to change with the length of active links.

#### D. Tissue-Inspired Programmable Material

Morpho modules can also be connected to form programmable material structure that was previously proposed in [12]. Fig. 12 (c) shows a basic cube of the programmable material, and Fig. 12 (d) demonstrates a programmable material that is formed by  $4 \times 4$  cubes. Same basic cube can be used to form other animal structures, e.g. robotic fish simulation in [27] use four cubes to form body of the fish.

### VI. POTENTIAL APPLICATIONS

We have shown several different types of shapes that can be achieved by this system, including time varying shapes and shapes that adapt to the environment. This can have many potential applications: a modular robot that is capable of squeezing its shape to fit through small spaces, a load bearing column that can expand in height, or a prosthetic device that adapts to fit a user's body and pattern of motion. In each case one can exploit both deformation and sensing to achieve shapes that are well suited to the environment parameters. The ability to create such adaptable programmable materials is a key area of future work

### VII. CONCLUSION

We have presented the design of the Morpho modular robot as well as different structures and shapes that it can achieve. The design of the robot is inspired by the Tensegrity model of cellular structure. In both hardware and simulation, we show that such a design can give rise to a variety of robotic and biological structures. In addition, the robot is capable of performing time-varying shape deformation tasks by controlling its active links.

In biological systems, self-assembly and cell reproduction often happen in the early process of development. After developing into mature organ or tissue, multi-cellular organisms usually perform self-deformation to achieve different tasks. In this paper, we show that self-deformation can be achieved by modular robotic systems. Morpho provides us with a useful platform to study the range of structures and shapes that are achievable with self- deformation. This will help us identify the most appropriate transformation approach - self-assembly, self-deformation or a hybrid approach that combines the two - for different classes of shape formation tasks on modular robots. In the future we plan to study this tradeoff between different types of shape formation as well as distributed control algorithms that allow us to create complex, adaptive, and dynamic shapes.

#### ACKNOWLEDGEMENT

We thank D. Kirk and I. Nishii for volvox inversion images (Fig. 2 (c)), M. Pickett for the artistic illustration of Tensegrity in the cell (Fig. 2 (b)), and anonymous reviewers for helpful comments. This work is partially funded by the NSF under Grant No. 0523676.

### REFERENCES

- [1] C.-H. Yu, F.-X. Willems, D. Ingber, and R. Nagpal, "Self-organization of environmentally-adaptive shapes on a modular robot," in *Proc. of Intl. Conf on Intelligent Robots and Systems (IROS 07)*, 2007.
- [2] V. Zykov, E. Mytilinaios, B. Adams, and H. Lipson, "Self-reproducing machine," *Nature*, vol. 435, no. 7038, pp. 163–164, 2005.
- [3] D. Rus, Z. Butler, K. Kotay, and M. Vona, "Self-reconfiguring robots," *Communications of the ACM*, vol. 45, no. 3, pp. 39–45, 2002.
- [4] J. Bishop, S. Burden, E. Klavins, R. Kreisberg, W. Malone, N. Napp, and T. Nguyen, "Self-organizing programmable parts," in *Proc. of Intl. Conf on Intelligent Robots and Systems*, 2006.
- [5] N. Wang, J. Butler, and D. Ingber, "Mechanotransduction across the cell surface and through the cytoskeleton," *Science*, vol. 260, pp. 1124–1127, May 1993.
- [6] D. Ingber, "The architect of life," *Scientific American*, pp. 48–57, Jan 1998.
- [7] L. Wolpert, R. Beddington, J. Brockes, T. Jessell, P. Lawrence, and E. Meyerowitz, *Principles of Development*. Oxford University Press, 1998.
- [8] A. Kamimura, E. Yoshida, S. Murata, H. Kurokawa, K. Tomita, and S. Kokaji, "A self-reconfigurable modular robot (mtran) - hardware and motion planning software," in *Proc. of DARS*, 2002.
- [9] W.-M. Shen, M. Krivokon, H. Chiu, J. Everist, M. Rubenstein, and J. Venkatesh, "Multimode locomotion for reconfigurable robots," *Autonomous Robots*, vol. 20, no. 2, pp. 165–177, 2006.
- [10] M. Yim, D. Duff, and K. Roufas, "Polybot: a modular reconfigurable robot," in *Proc. of Intl. Conf on Robotics and Automation*, 2000.
- [11] K. Stoy, A. Lyder, R. Garcia, and D. Christensen, "Hierarchical robot," in *Proc. of IROS Workshop on Self-Reconfigurable Robots/Systems and Applications*, 2007.
- [12] R. Nagpal, "Programmable self-assembly using biologically-inspired multiagent control," in *Proc. of AAMAS*, 2002.
- [13] R. Schmitt and M. Sumper, "Developmental biology: How to turn inside out," *Nature*, vol. 424, pp. 499–500, 2003.
- [14] G. Odell, G. Oster, P. Alberch, and B. Burnside, "The mechanical basis of morphogenesis, 1. epithelial folding and invagination," *Developmental Biology*, vol. 85, 1981.
- [15] J. M. Anderson and N. K. Chhabra, "Maneuvering and stability performance of a robotic tuna," *Integrative and Comparative Biology*, vol. 42, pp. 118–126, 2002.
- [16] H. Yamada, S. Chigisaki, M. Mori, K. Takita, K. Ogami, and S. Hirose, "Development of amphibious snake-like robot acm-r5," in *Proc. of 36th International Symposium on Robotics*, 2005.
- [17] M. Vona and D. Rus, "Crystalline robots: Self-reconfiguration with compressible unit modules," *J. of Autonomous Robots*, vol. 10, 2001.
- [18] G. J. Hamlin and A. C. Sanderson, *Tetrobot A Modular Approach to Reconfigurable Parallel Robotics*. Springer, 1997.
- [19] K. Støy, "The deformatron robot: a biologically inspired homogeneous modular robot," in *Proc. of ICRA*, 2006.
- [20] J. Aldrich, R. Skelton, and K. Kreutz-Delgado, "Control synthesis for a class of light and agile robotic tensegrity structures," in *Proc. of American Control Conference (ACC)*, 2003.
- [21] C. Paul, F. Valero-Cuevas, and H. Lipson, "Design and control of tensegrity robots for locomotion," *IEEE Trans. on Robotics*, 2006.
- [22] S. Murata, E. Yoshida, A. Kamimura, H. Kurokawa, K. Tomita, and S. Kokaji, "M-tran: Self-reconfigurable modular robotic system," *IEEE/ASME Trans. Mechatron*, vol. 7, no. 4, pp. 431–441, 2002.
- [23] S. C. Goldstein, J. Campbell, and T. C. Mowry, "Programmable matter," *IEEE Trans. Comput.*, vol. 38, no. 6, pp. 99–101, 2005.
- [24] Y. Yoon and D. Rus, "Shady3d: A robot that climbs 3d trusses," in *Proc. of Intl. Conf on Robotics and Automation*, 2007.
- [25] C.-H. Yu and R. Nagpal, "Sensing-based shape formation tasks on modular multi-robot systems: A theoretical study," in *Proc. Intl. Conf on Autonomous Agents and Multi-Agent Systems (AAMAS)*, 2008.
- [26] T. Umedachi, T. Kitamura, and A. Ishiguro, "A fully decentralized control of an amoeboid robot by exploiting the law of conservation of protoplasmic mass," in *Proc. of ICRA*, 2008.
- [27] X. Tu and D. Terzopoulos, "Artificial fishes: Physics, locomotion, perception, behavior," in *Proc. of ACM SIGGRAPH*, 1994.